



**University of Leipzig
Faculty of Physics and Earth Sciences
Advanced practical course in physics**

Protocol

Rotational vibration spectra of molecules

Submitted by: xxxx
Pascal Schumann

Supervisor: Dr. Chris Sturm
Faculty of Physics and Earth Sciences

Experiment: 24.10.2023

Delivery: 20.11.2023

Table of contents

1 Theoretical preliminary consideration	1
1.1 FTIR spectroscopy.....	1
1.2 Rotational vibration spectra of 2-atom molecules.....	3
1.3 Interference method for coating thickness determination and the Fabry-Pérot interferometer	7
1.3.1 Interference on thin films.....	7
1.3.2 The Fabry-Pérot interferometer.....	8
1.4 Intensity of the rotational vibration spectrum.....	9
2 Experimental setup	11
3 Task	13
4 Evaluation Task 1	15
4.1 Water vapor.....	15
4.2 Polystyrene	16
5 Evaluation of task 2	17
5.1 Calibration	17
5.2 Zerofilling	19
5.3 Apodization.....	20
5.4 Comparison of two special settings	21
5.5 Theoretical resolution.....	22
6 Evaluation of task 3	23
6.1 Glass blocking filter	23
6.2 NaCl blocking filter	24
7 Evaluation of task 4	25
8 Evaluation of task 5	27
9 Evaluation of task 6	31
10 Bibliography	33

1 Theoretical preliminary consideration

1.1 FTIR spectroscopy

First, some basics of FTIR spectroscopy will be considered. It is used to investigate various physical properties of substances or to determine unknown substances using characteristic spectra. The *Spectrum 100* spectrometer used by PerkinElmer works on the principle of a Michelson interferometer, which is why it is briefly described below.

A blackbody radiator is used in the spectrometer. This emits a beam of light which hits a semi-transparent mirror that acts as a beam splitter. The first partial beam always follows the same path, where it is reflected by a mirror and then hits the sample before entering the detector. However, interference with the second partial beam, which was previously reflected by a moving mirror and therefore has a variable path difference to the first partial beam, already occurs before the sample. The spectrometer records the intensity of the transmitted light as a function of the travel distance of the mirror apparatus. This is referred to as an interferogram, which must be converted into a spectrum using a Fourier transformation. FTIR spectrometers have a very high wavenumber accuracy, which is just a few cm^{-1} .

Several methods are used to increase the quality of the spectrum display:

1. Apodization: Apodization converts the sudden interruption of the interferogram into a steady drop, which is achieved by multiplication with a makeshift function. This can reduce a disturbance of the spectrum, the so-called leakage effect. Depending on which function is used for multiplication, the drop is then more or less steep. However, the stronger the apodization function used, the poorer the resolution of the spectrum will ultimately be.

2. Zerofilling: With zerofilling, the measured data is supplemented by many zeros, which leads to more points in the display and thus to a smoother display.

1. theoretical preliminary consideration

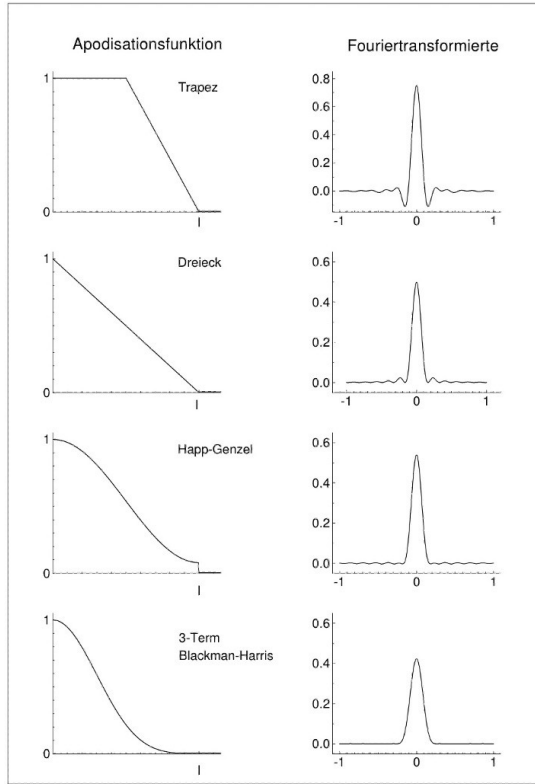


Figure 1.1: Examples of apodization functions (Riede n.d.)

curve. The so-called picket fence effect, in which transmission minima are less easily recognized or not recognized at all due to excessive distances between the points, is thus reduced. However, the amount of information in the measurement is not improved by zero-filling, only the number of points displayed in the spectrum.

3. Phase correction: The Fourier transformation first transforms the unidirectional interferogram into a complex spectrum, which is then converted back into a real spectrum by phase correction.

Once the spectrum has been created, it must be divided by a reference spectrum in order to obtain the correct measured values for the respective sample.

1.2 Rotational vibration spectra of 2-atom molecules

1.2 Rotational vibration spectra of 2-atom molecules

In molecules consisting of two atoms, there is often a dipole moment along the axis connecting the two atoms. The absorption in the infrared range is caused by the different rotations and vibrations of the molecules, which change the electric dipole moment. In very simplified terms, the molecule can be viewed using the dumbbell model, in which the masses of the atoms are assumed to be point masses that rotate at a fixed distance around a fixed axis through the center of gravity.

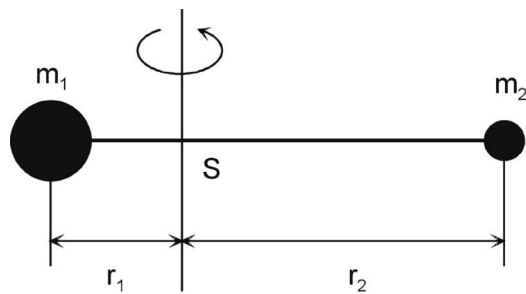


Figure 1.2: Dumbbell model (Riede (n.d.)

The dumbbell has the moment of inertia

$$I = \mu - r_0^2 , \quad (1.1)$$

where for the reduced mass

$$\mu = \frac{m_1 \cdot m_2}{m_1 + m_2} \quad (1.2)$$

applies. After solving the Schrödinger equation in polar coordinates and vanishing potential, the discrete energy values are obtained

$$E_m = m \frac{h^2}{8\pi^2 \mu r_0^2} . \quad (1.3)$$

In the following, this dumbbell can then be considered with the rotation around a space-free axis, whereby the transition from polar to spherical coordinates makes sense. In this case, the energy

1. theoretical preliminary consideration

$$E(J) = hcBJ(J+1); J \in \mathbb{N}_0 \quad (1.4)$$

with the rotation constant

$$B = \frac{\hbar}{8\pi^2 c I}. \quad (1.5)$$

The rotation term thus results in

$$F(J) = \frac{E}{hc} = BJ(J+1); J \in \mathbb{N}_0 \quad (1.6)$$

with the selection rule

$$\Delta J = \pm 1. \quad (1.7)$$

In addition, the harmonic oscillator can be considered, initially in isolation.

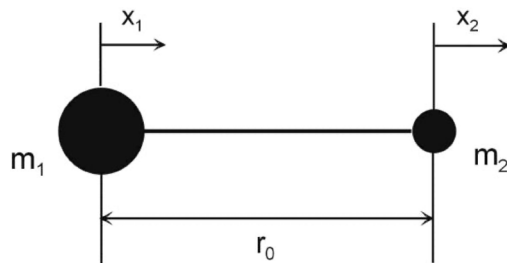


Figure 1.3: 2-atom molecule as a harmonic oscillator (Riede n.d.)

1.2 Rotational vibration spectra of 2-atom molecules

Here, the equations of motion are obtained by considering the forces

$$m_1 \ddot{x}_1 = -k(x_1 - x) \quad (1.8)$$

$$m_2 \ddot{x}_2 = -k(x_2 - x_1), \quad (1.9)$$

which can be converted

via $x_1 - x_2 = x$ to

$$\ddot{x} = -\frac{k}{\mu}x \quad (1.10)$$

can be summarized. The resonance wave number of such a harmonic oscillator is then

$$\nu_s^{-} = \frac{1}{2\pi c} \sqrt{\frac{k}{\mu}}. \quad (1.11)$$

To calculate the energy values here too, solve the Schrödinger equation for the potential

$$U = 2\pi c^2 \nu_s^{-2} \mu x^2, \quad (1.12)$$

which is derived from the back-driving force via

$$-\frac{dU}{dx} = F = -\frac{k}{x} \quad (1.13)$$

with the
approach

$$x = x_0 \sin(2\pi c \nu_s^{-} t) \quad (1.14)$$

is obtained. This also provides discrete energy levels

$$E(n) = \frac{\hbar c \nu_s^{-}}{2} n + \frac{1}{2}; \quad n \in \mathbb{N}, \quad (1.15)$$

with the selection rule

$$\Delta n = \pm 1. \quad (1.16)$$

1. theoretical preliminary consideration

These energy levels in turn provide the oscillation term

$$G(n) = \frac{E(n)}{hc} = \nu^-_s + \frac{n + \frac{1}{2}}{2} . \quad (1.17)$$

Both effects can now be combined to obtain the rotational vibration spectra. If interactions are initially neglected, the rotational and vibrational energy add up to

$$E(n, J) = hcBJ(J+1) = \nu^-_s + \frac{n + \frac{1}{2}}{2} . \quad (1.18)$$

and you get the rotational oscillation term

$$T(n, J) = \frac{E(n, J)}{hc} = BJ(J+1) + \nu^-_s + \frac{n + \frac{1}{2}}{2} . \quad (1.19)$$

Transitions are possible for

$$\Delta J = \pm 1 \text{ and } \Delta n = 0, \pm 1. \quad (1.20)$$

The transitions can be divided into the R branch with an increase in J and the P branch, where J decreases. A pure rotation spectrum is obtained for the transitions with $n = \text{const}$. For additional consideration of the interactions between oscillation and rotation, one must first switch from the dumbbell model to the non-rigid rotator, which results in the oscillation term as a function of the quantum number as follows

$$F_n(J) = B_n J(J+1) - D_n J_n^2 (J+1)^2 , \quad (1.21)$$

where D_n is the respective strain constant. The reason for the n-dependence lies in the change in the mean distance between the atoms. If each transition is given an index i ($i = \Delta J$), a relationship between the respective wavenumber of the minimum and the quantum number-dependent rotation and strain constants can be specified with

$$\nu^- = \nu^-_s + (B_1 + B_0)i + (B_1 - B_0)t^2 - 2(D_1 + D_0)t^3 . \quad (1.22)$$

1.3 interference method for layer thickness determination and the Fabry-Pérot interferometer

If we calculate the difference between two neighboring wave number minima and the difference between them, we obtain the following equations

$$\Delta v^-(i) = 2B_1 - 2(D_1 + D_0) + 2i(B_1 - B_0 - 3(D_1 + D_0)) - 6i^2(D_1 + D_0) \quad (1.23)$$

$$\Delta(\Delta v^-(i)) = 2(B_1 - B_0) - 12(D_1 + D_0) - 12i(D_1 + D_0). \quad (1.24)$$

If a linear fit is carried out for the second equation, $(D_1 + D_0)$ results from the rise and $(B_1 - B_0)$ then from the *y-intercept*. B_1 and B_0 can then be calculated using equation (1.23).

1.3 Interference method for determining coating thickness and the Fabry-Pérot interferometer

1.3.1 Interference on thin layers

To understand the Fabry-Pérot interferometer, you should first have some basic knowledge of interference on thin layers. If light is transmitted through a cuvette, reflection at the boundary layers between the glass and the filler causes interference between the initially reflected and the directly transmitted waves, as can be seen in the figure.

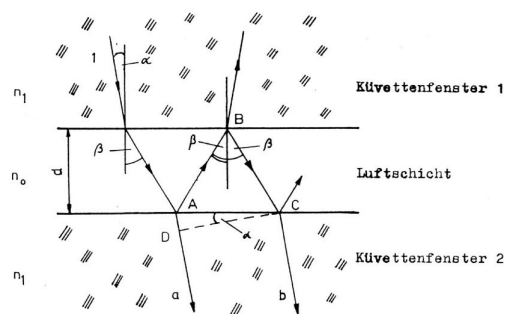


Figure 1.4: Interference on thin layers during transmission (Riede (n.d.)

Whether this interference is constructive or destructive depends on the path difference of the waves.

1. theoretical preliminary consideration

This amounts to

$$\Delta = n_0 (AB + BC) - n_1 AD \quad (1.25)$$

and can be calculated using trigonometric relationships and Snellius' law of refraction

$$\frac{n_1}{n_0} = \frac{\sin \beta}{\sin \alpha} \quad (1.26)$$

transform to

$$\Delta = 2n_0 d \cos \beta. \quad (1.27)$$

Destructive interference occurs when the path difference is a half-integer multiple of the wavelength and constructive interference occurs accordingly for all integer multiples. The difference between the ordinal numbers of the maxima is

$$N_1 - N_2 = 2dn_0 (\nu^-_1 - \nu^-_2), \quad (1.28)$$

which results in the film thickness for an air-filled cell ($n_0 \approx 1$) being

$$d = \frac{N_1 - N_2}{2(\nu^-_1 - \nu^-_2)} \quad (1.29)$$

results

This section is not relevant,
does not have to be included in the
preparation

1.3.2 The Fabry-Pérot interferometer

The Fabry-Perot interferometer has the special feature that it generates the interference through a so-called etalon, i.e. two parallel glass plates or a glass block, in which the light is reflected very often and the small part that is transmitted with each reflection interferes. Due to deviations from the optical axis, the angle of incidence and thus also the path differences in the interference on the thin layer vary, whereby the interference maxima appear as rings that become narrower and weaker towards the outside. In addition, the path difference can be varied by the distance between the glass plates. In comparison to the Michelson interferometer, the beam splitter is not necessary in this case, as the glass plates act as a mirror and beam splitter in one. This means that the interference on thin

1.4 Intensity of the rotational vibration spectrum

layers and their dependence on the angle of incidence, which has already been explained. The transmission of the etalon depends on the wavelength, the angle of incidence, the thickness of the etalon and its refractive index and can be determined by

$$T = 1 + \frac{4r}{(1 - r)^2} \sin^2 \frac{\delta}{2} \quad (1.30)$$

can be calculated. Where r stands for the reflectivity of the individual surfaces and

$$\delta = \frac{2\pi}{\lambda} 2nd - \cos(\Theta) \quad (1.31)$$

with the angle Θ between the waves and the optical axis.

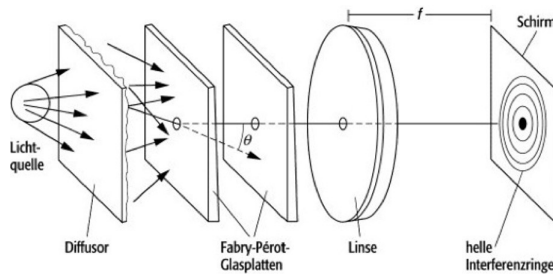


Figure 1.5: Structure of a Fabry-Pérot interferometer (spectrum)

1.4 Intensity of the rotational vibration spectrum

If we consider the number of molecules N , which are in the state with $n = 0$ you will find

$$N(J, n=0) = \frac{\frac{N_{ges}}{Q} (2J+1) \exp - \frac{hcBJ(J+1)}{kT_r}}{\exp - \frac{hc\bar{v}}{kT}} \quad (1.32)$$

with Q_r the sum of states. For the absorption coefficient, which is decisive for the intensity of the minima, this results in

1. theoretical preliminary consideration

$$\alpha = c_3 \bar{v} (2J+1) \exp \left(-\frac{hcBJ(J+1)}{kT} \right) , \quad (1.33)$$

where c_3 is a constant. Using Lambert-Beer's law, the relative intensities are given by

$$I(J) = I_0 \exp(-\alpha d) = I_0 \exp \left(-\frac{hcBJ(J+1)}{kT} \right) , \quad (1.34)$$

where ν^- is given by (1.22).

2 Experimental setup

The *Perkin Elmer Spectrum 100 FTIR spectrometer* was used in the experiment. The mode of operation is based on a modified Michelson interferometer, in which the change in the path difference between the two light beams is realized by rotating an additional pair of mirrors around a common axis.

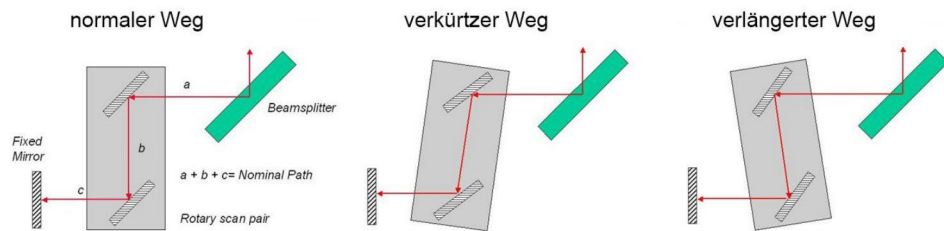


Figure 2.1: Realization of the path difference via rotatable mirror apparatus

A so-called "glowbar" is used as the light source. This is a silicon carbide crystal through which a current flows. This heats the crystal and subsequently emits an almost perfect blackbody spectrum, which has its maximum in the mid-infrared.

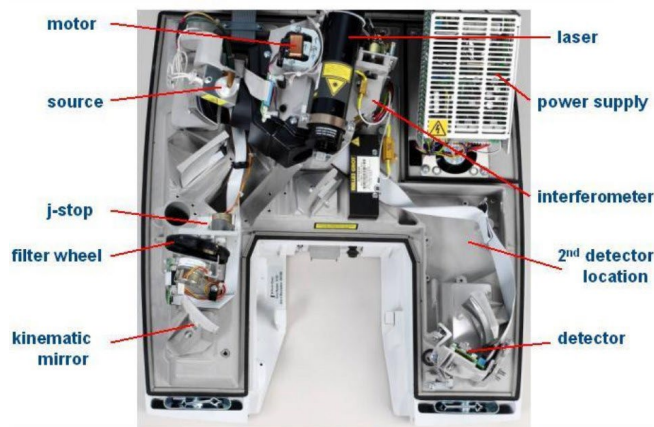
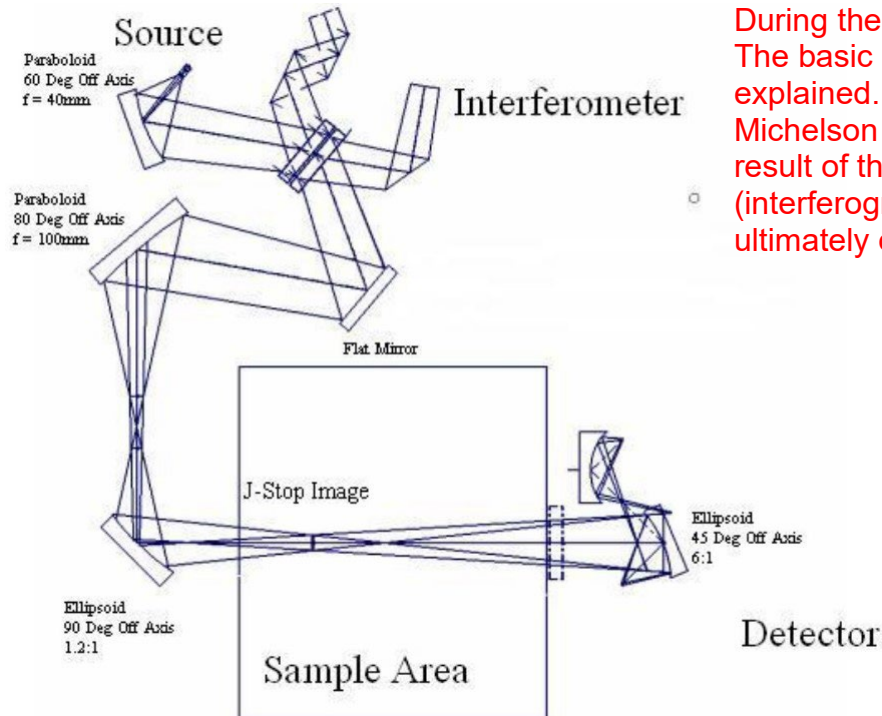


Figure 2.2: Structure inside the *Spectrum 100* spectrometer

2. experimental setup



During the test, the basic structure was explained. It was mainly about the Michelson interferometer and the result of the measurement (interferogram). How do you ultimately obtain the spectrum?

Figure 2.3: Schematic of the optics inside the spectrometer

For the measurement, the respective sample is placed in the cuvette holder of the device. After closing the lid and starting the measurement, the spectrometer records an interferogram. The travel distance of the mirror apparatus can also be selected. Depending on the type of measurement selected, the spectrum is either generated by the device itself or calculated manually using a Fourier transformation, e.g. in the *Origin Lab* software.

3 Task

Task 1

Check the calibration of the wavenumber scale of the Spectrum 100 infrared spectrometer using the polystyrene and water vapor bands. The deviations determined experimentally are to be displayed graphically and discussed.

Task 2

Interferograms of the water vapor spectrum are to be recorded at different operating ranges of the interferometer. A Fourier transformation of these interferograms must then be carried out. Calibrate the wavenumber scale using the known water vapor modes. Determine the step size of the optical path difference between the individual measuring points from the bandwidth of the spectrum. Discuss the influence of travel distance, zero-filling and apodization on the resolution on the basis of the spectra. The theoretical resolving power must be specified using the calculated step size as a function of the number of points.

Task 3

Use glass plate and NaCl blocking filters to determine the displayed signal strength in the blocking range of the filters.

Task 4

Determine the film thickness of a liquid cuvette using the interference method. A graph ΔN over v^-_N must be prepared. The layer thickness and its mean square error must be determined using the equalization calculation.

3. task definition

Task 5

Record the rotational vibration spectrum of hydrogen chloride (HCl gas) at a suitably selected resolution and determine the wavenumbers of the bands. The values are to be corrected according to the calibration measurements. The vibrational wavenumber, the force constant, the rotational constant, the distance between the two atoms and the moment of inertia of the HCl molecule as well as the corresponding errors must be calculated. In addition, the vibration-dependent rotational constant B_n , the strain constant D and the splitting caused by the isotopes must be determined experimentally and calculated. The ratio of the isotopes must be calculated from the spectra in accordance with the Lambert-Beer law.

Task 6

The intensities of the absorption minima of the P-branch are to be modeled on the basis of the theoretical absorption coefficient. The temperature of the gas is to be determined from the model as a free parameter of the fitting.

4 Evaluation of task 1

For the two measurements of water vapor and polystyrene, the spectrum was displayed and then the minima given from the test documents were entered and compared with the actual measurements. The transmission is given in the graphs in arbitrary units. The deviations were determined from the comparison in order to be able to draw conclusions about the calibration of the device.

4.1 Water vapor

When measuring the spectrum of water vapor, the cuvette holder was left empty. Instead, the water vapor present in the room air can be used. Only the wave numbers in the relevant range (presence of calibration bands) were shown in the graph.

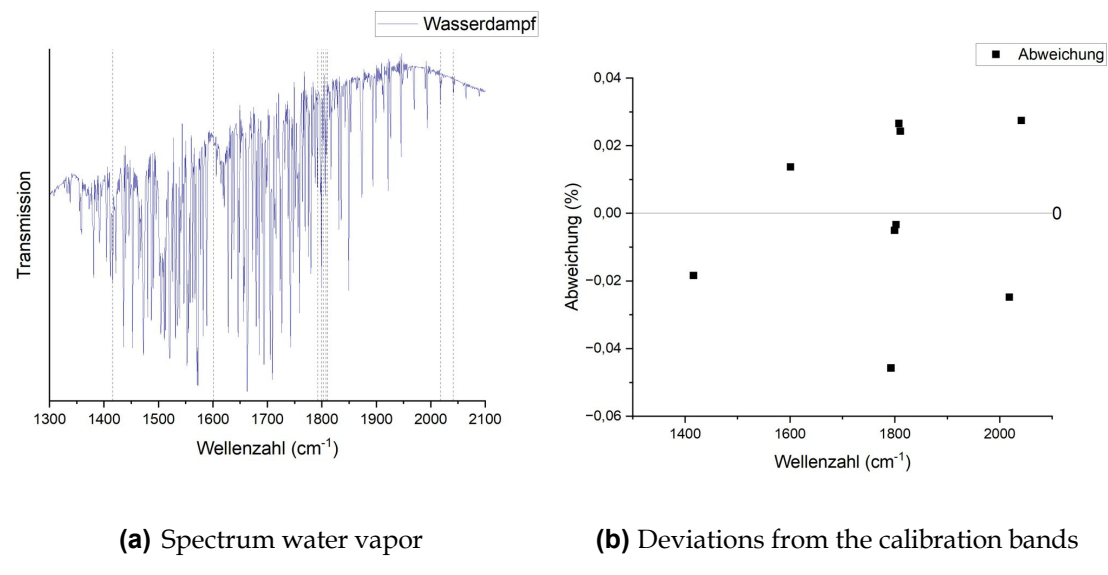


Figure 4.1: Calibration with water vapor calibration bands

The positions of the minima, which belong to the respective calibration band, are easy to recognize in the graph. The calibration of the spectrometer is very good. He wanted to know whether the deviation was dependent on the device or the sample.

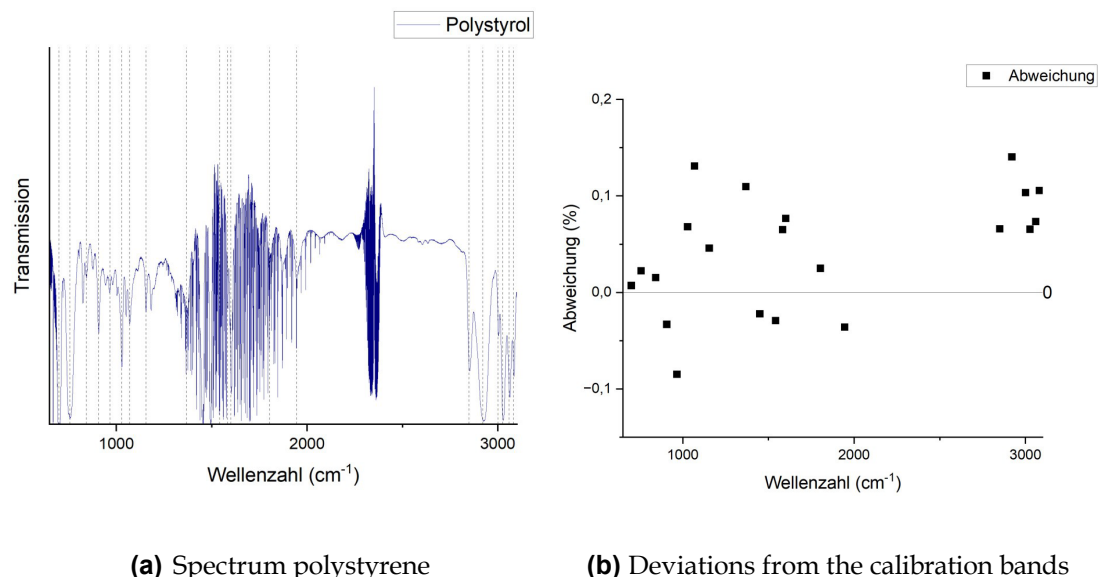
(they are device-dependent). Accordingly, the deviations from the calibration bands should be included in a common diagram, as the error should be approximately the same for both samples and an average value can therefore be taken over more individual values.

4. evaluation of task 1

as the deviations of the measurement are only minor. The standard deviation of the absolute deviation is around 0.48 cm^{-1} , while the same is around 0.026 % for the relative values.

4.2 Polystyrene

To measure the spectrum of polystyrene, the measured values recorded must be standardized due to the water vapour present in the room air. Only the relevant wave numbers and the positions of the calibration bands are shown in the graph.



(a) Spectrum polystyrene

(b) Deviations from the calibration bands

Figure 4.2: Calibration with polystyrene calibration bands

The differences between the minimum and the respective calibration band can be clearly seen in the graph. This can also be seen in the deviations. The standard deviations are 1.37 cm^{-1} or 0.061 %. This is also within an acceptable range. The higher error can be explained by the standardization. Two measurements were carried out to create the spectrum, both of which contribute their own errors, resulting in larger shifts in the minima compared to the calibration bands. For further considerations, the deviations of the polystyrene measurements are used as errors, as all other measurements must also be normalized.

5 Evaluation of task 2

Interferograms of the water vapor were recorded with different travel distances of the spectrometer's mirror apparatus. The spectrum was then calculated using a Fourier transformation. The influences of travel distance, apodization and zerofilling were investigated.

The travel distance describes the number of data points that are recorded by the spectrometer. The highest possible resolution can be achieved with the setting -8000 to 32000. Consequently, 40001 data points are recorded here.

5.1 Calibration

In order to be able to correctly transfer the data from the Fourier transformation into a spectrum, a calibration was first carried out, which can then be used for all interferograms. The range -8000 to 8000 was used for this. The following interferogram and its Fourier transform are obtained.

If he wants to know why the peak at $x=0$ is so large: There is no peak there. path difference and thus all wavelengths interfere constructively

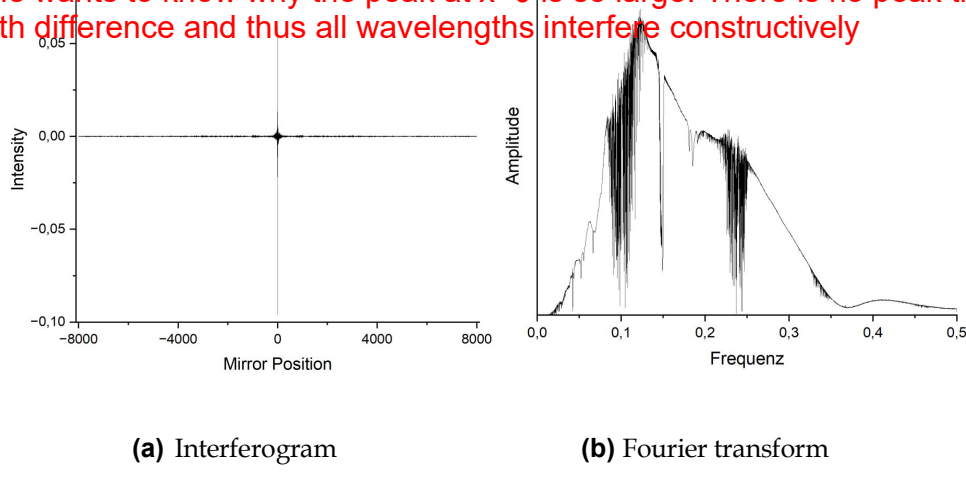


Figure 5.1: Calibration measurement

First he wanted to know what the interferogram of monochromatic light looks like (it is not a sine wave) function, but its square, because the intensity is the square of the wave function - therefore the intensity never becomes negative). He then wanted to know why the "intensity" in the diagram becomes negative. To do this, you have to look at how the intensity is constructed. It is calculated from the complex wave function of the superposition of both partial waves and is therefore $I_{ges}^2 = I_1^2 + I_2^2 + 2\cos(\phi) \cdot I_1 \cdot I_2$. The phase-dependent term, which results from the superposition of the complex partial waves, is obviously also negative. What you see in the interferogram is only the phase-dependent term, because the constant intensities I_1 and I_2 are not of interest for the Fourier transform.

5. evaluation of task 2

No apodization (rectangular function) or zerofilling was used for the Fourier transformation. As can be seen in the graph, the *Origin Lab* application outputs frequencies in the range from 0 to 0.5 by default. Consequently, the x-axis still needs to be scaled. For this purpose, an enlarged section of the Fourier transform was considered.

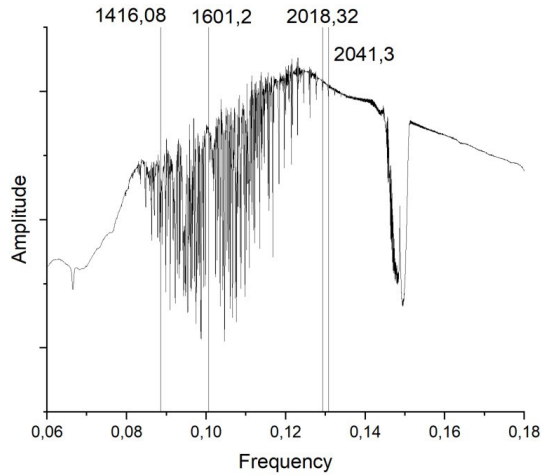


Figure 5.2: Enlarged section of the Fourier transforms

This makes it easier to identify distinctive minima. For this purpose, the section was compared with the measurement of the single-channel spectrum and the wavenumber of the calibration band marked in the graph was determined. The two calibration bands with the smallest or largest wavenumbers were used in each case in order to cover as large a range as possible. The equation for scaling the *x-axis* can be determined using a linear fit.

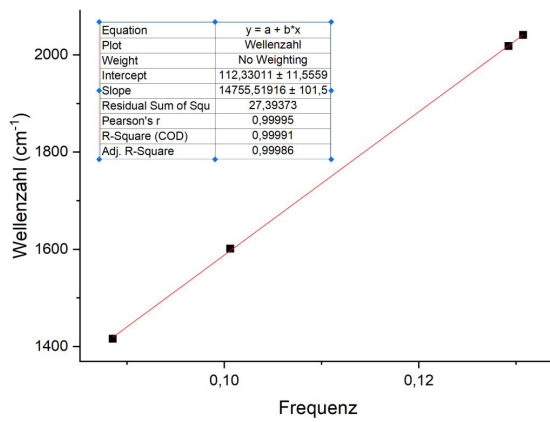


Figure 5.3: Linear fit for scaling the x-axis

5.2 Zerofilling

Again, as in task 1, there is a very small error in the measurement compared to the calibration bands. Applying the calibration and scaling finally results in the spectrum.

The Mertz method was used in all cases to determine the amplitude of the spectrum.

5.2 Zerofilling

The spectra for no zerofilling, weak zerofilling (factor $a = 2$) and strong zerofilling (factor $a = 6$) are compared below. The measured values for the travel distance -8000 to 8000 were used for this.

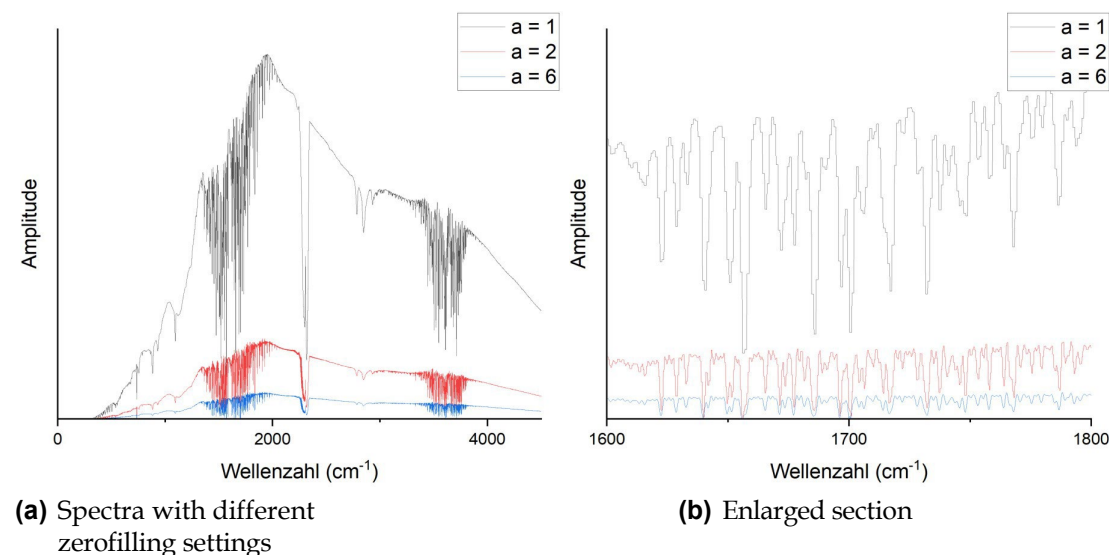


Figure 5.4: Influence of zerofilling

It can be clearly seen that larger zerofilling factors reduce the amplitude. The enlarged section shows that in the absence of zerofilling, closely spaced minima can sometimes no longer be recognized individually, which with stronger zerofilling can be recognized as two individual minima.

nima (see, for example, $\nu^- \approx 1720 \text{ cm}^{-1}$). Nevertheless, one can do not increase the zerofilling factor indiscriminately, as a higher factor also causes a smoothing of the graph, which can lead to a point where a minimum can no longer be recognized as such. The average factor of $a = 2$ seems to be the best decision between the three available options (especially for the selected travel distance).

5. evaluation of task 2

5.3 Apodization

For apodization, spectra of two different travel distances are considered, as the leakage effect, which apodization attempts to prevent, occurs differently at different resolutions. The interferograms were multiplied with a rectangular function, triangular function or the Blackman function before the Fourier transformation. Initially, a very low range of -1000 to 1000 was selected.

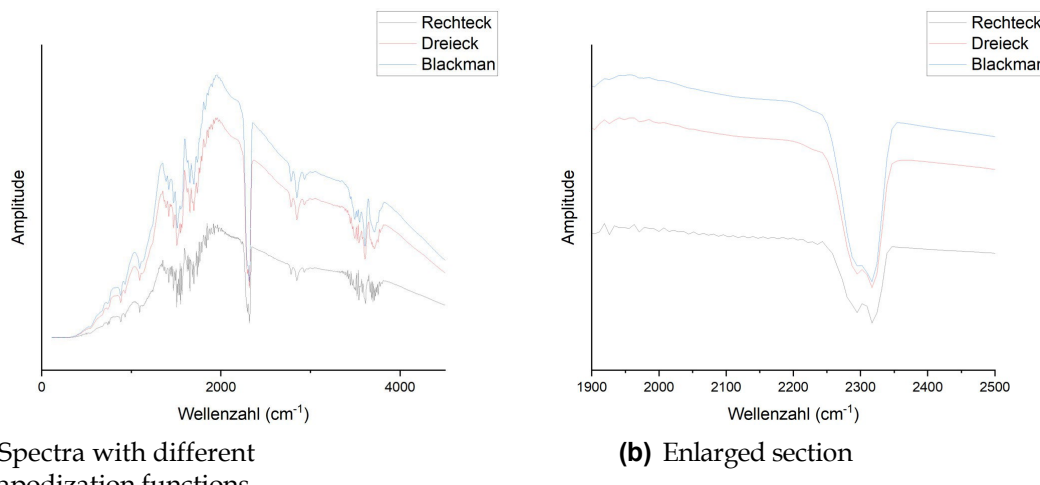


Figure 5.5: Travel range -1000 to 1000

The enlarged section clearly shows that the leakage effect has been reduced - particularly with the help of the Blackman function. At the point $\nu^- \approx 2300$ cm⁻¹ it can be assumed that two minima are close together here. This is difficult to recognize due to the low resolution in the rectangular spectrum. Due to the apodization, this can no longer be seen in the Blackman spectrum, for example. This shows a disadvantage of apodization at low resolutions (travel distances).

Furthermore, the maximum range of the spectrometer was used with -8000 to 32000. Data points that were only available on one side were supplemented by mirroring at $x = 0$ before the Fourier transformation.

There is no significant advantage of stronger apodization with regard to the leakage effect. On the contrary, there is a certain roughness in the data. The increase in the widths of the minima can also be seen - even if this effect is only minimal.

He wanted to know what effect there is due to the fact that the interferogram is infinite or breaks off (A: leakage effect). How does this affect the spectrum and how can it be prevented? What happens in the spectrum with increasing apodization and does apodization improve the resolution?

5.4 Comparison of two special settings

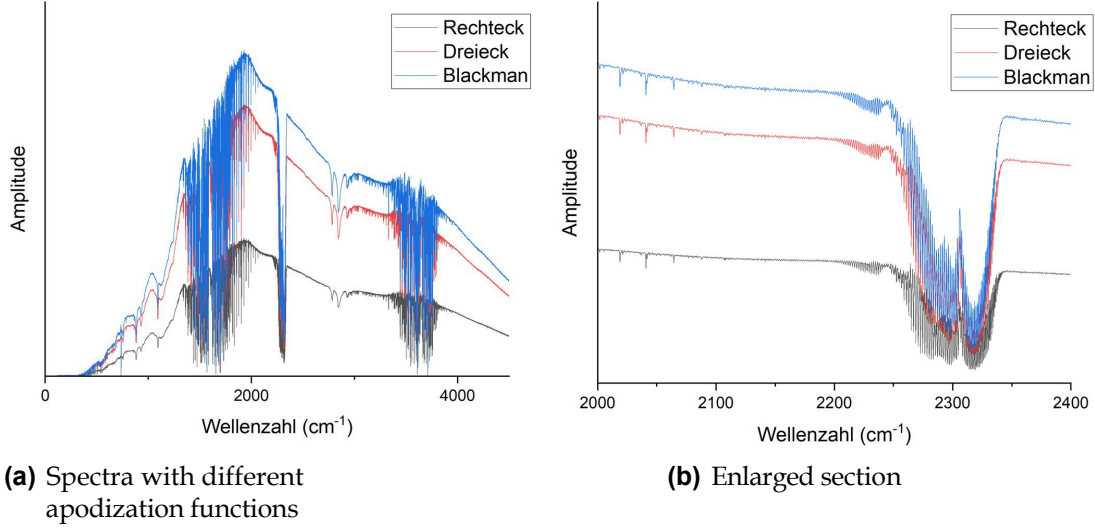


Figure 5.6: Travel range -8000 to 32000

5.4 Comparison of two special settings

Finally, two special settings are considered. Setting a) comprises a travel range of -8000 to 32000, no zero filling and strong apodization (Blackman function). Setting b) comprises a travel range of -8000 to 8000, zero filling with the factor $a = 4$ and no apodization (rectangular function).

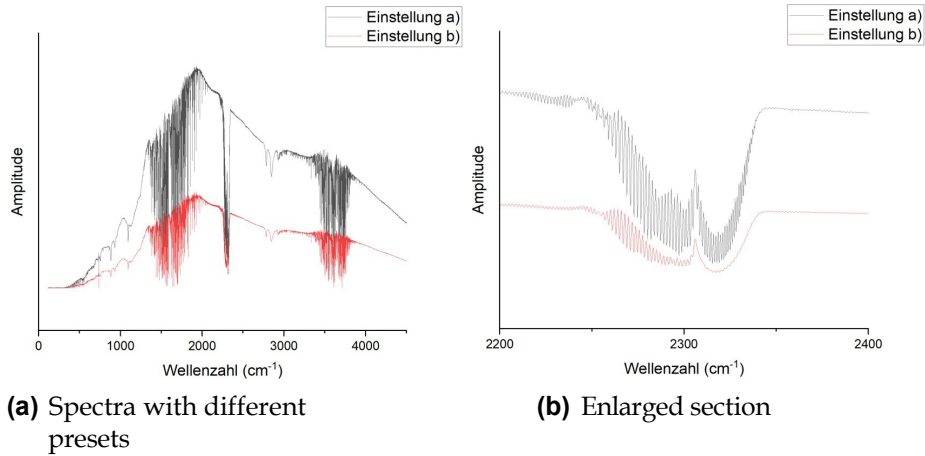


Figure 5.7: Comparison of the two settings a) and b)

5. evaluation of task 2

It is very clear to see that, as expected, the spectrum is somewhat smoother at setting b) - at setting a), more individual peaks can be seen that would otherwise not be recognizable. This is mainly due to the higher resolution at a), which cannot be achieved in b) even with zero filling. However, in both spectra it is sometimes relatively difficult to determine which minima are actually present and which are due to the leakage effect.

5.5 Theoretical resolution

The spectrometer operates in the mid-infrared, i.e. at wavelengths of approximately $2.5 \text{ } \mu\text{m}$ to $50 \text{ } \mu\text{m}$, which corresponds to a maximum wavenumber of $\nu^{-}_{max} = 4000 \text{ cm}^{-1}$. Consequently, the measuring points of the interferogram have a distance of

$$\Delta x = \frac{1}{2 \frac{1}{\nu^{-}_{max}}} = 1,25 \cdot 10^{-4} \text{ cm.}$$

This results in a theoretical resolution as a function of the number of measuring points n of

$$\Delta \nu^{-} = \frac{1}{n \cdot 1,25 \cdot 10^{-4} \text{ cm}}.$$

6 Evaluation of task 3

First, the blocking range of the respective filters must be determined in order to then be able to determine the signal strength there.

6.1 Glass blocking filter

Glass blocks in a wavenumber range below $\nu_{max}^- \approx 2100 \text{ cm}^{-1}$. A lower limit cannot be determined as the wavelength range of the spectrometer does not extend into the far infrared and the accuracy decreases significantly for smaller wavenumbers as can be seen in the graph. The transmission in the blocking range is in the order of 10^{-4} to 10^{-3} .

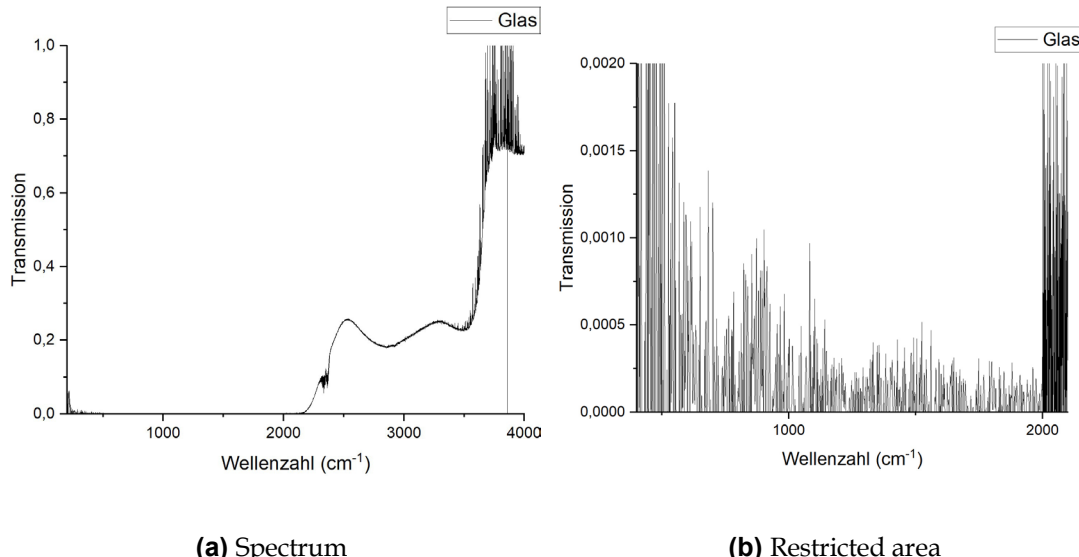


Figure 6.1: Glass blocking filter

The labeling of the y-axis should not be transmission but "transmittance", because it is ultimately standardized to the background (water vapour).

6. evaluation of task 3

6.2 NaCl blocking filter

The NaCl filter blocks in a wavenumber range below $\nu_{max}^- \approx 500 \text{ cm}^{-1}$. A lower limit cannot be determined for the same reasons as above. The transmission in the blocking range is in the order of 10^{-3} to 10^{-2} . This is significantly greater (factor 10) than with glass, which means that the glass blocking filter is also more effective at blocking the light.

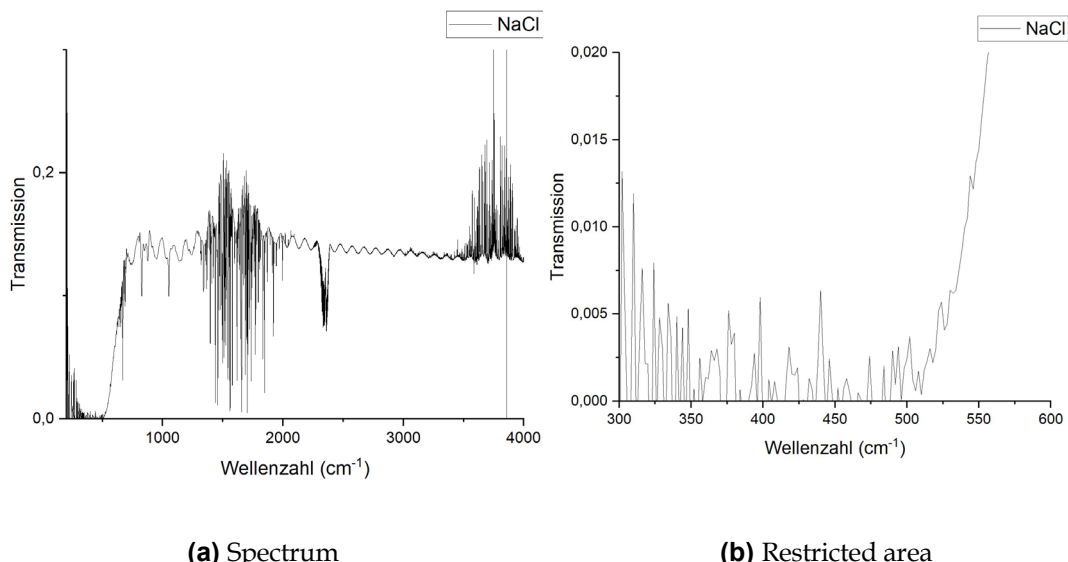


Figure 6.2: NaCl blocking filter

This diagram shows strong noise in the non-locking range. This is due to
This is due to the fact that the NaCl spectrum was carried out using a single-channel
measurement and the background (water vapor) was calculated using the interferogram. This
results in noise due to the different settings. This should not happen and in our case was due to a
faulty data set of the single-channel spectrum of water vapor.

In the stopband, large deflections can be seen at low wave numbers (below 350 cm(-1)). Why
(A: This is due to the fact that the barrier filters and the background (water vapor) become very
small in this area. Accordingly, even the smallest fluctuations have a very strong effect and the
observed deflections occur)

7 Evaluation of task 4

The spectrum was normalized and then displayed in a range in which there is little noise. A total of 9 minima were marked, from which the film thickness of the KBr cell can be determined with the aid of the equalization calculation and using the equation (1.29).

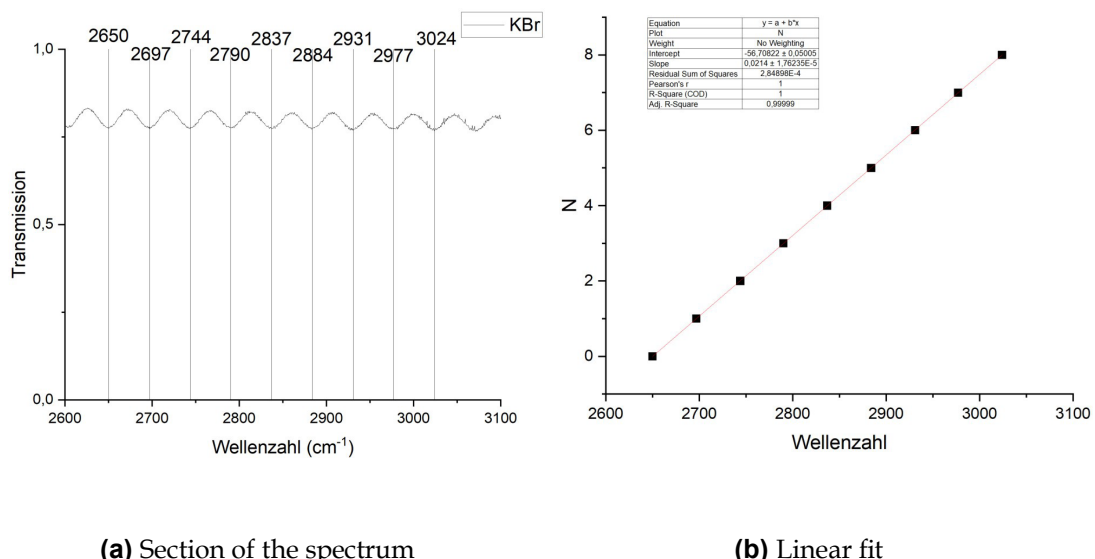


Figure 7.1: Empty KBr cuvette

The increase determined from the equalization calculation corresponds exactly to twice the layer thickness d to be determined. The final result is $d = (107, 00 \pm 0, 09) \mu\text{m}$.

Here it should be explained how the minima and maxima in the diagram come about (keyword: Interference on thin layers, a few more notes on the path difference and the course of the rays at the different orders of maxima and minima).

Caution: Phase jumps occur during reflection on the optically denser medium (occurs 2 times during transmission - for order 1 - and thus cancels itself out, so need not be taken into account)

8 Evaluation of task 5

Chlorine has the two isotopes³⁵ Cl and³⁷ Cl, which is why a splitting of the minima of the P and R branches can be seen in the spectrum of HCl. The left minimum belongs to the isotope³⁷ Cl and the right minimum to the isotope³⁵ Cl. This results in the following spectrum with the corresponding measured values.

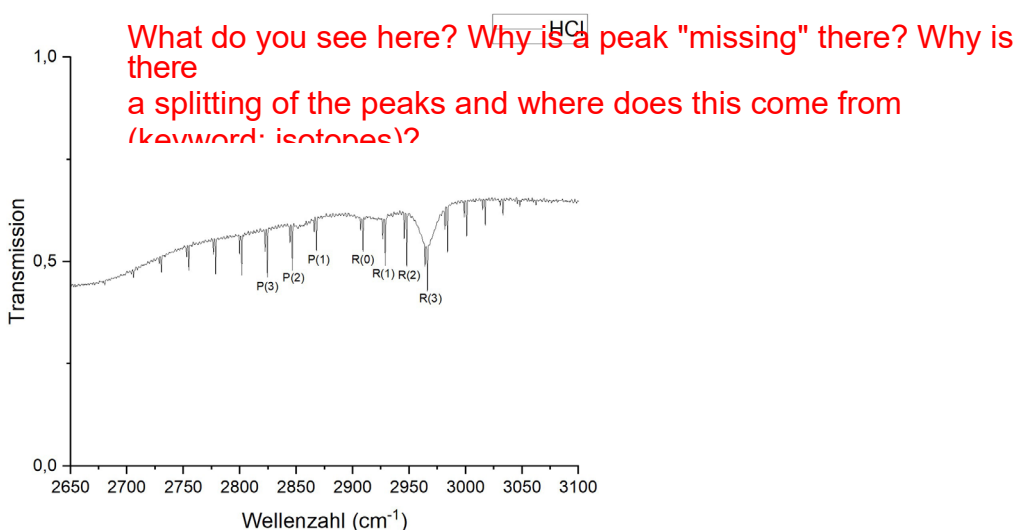


Figure 8.1: Enlarged section of the HCl spectrum

Minimum	Index i	$\nu^{-}(\text{Cl}^{35}) [\text{cm}^{-1}]$	$\nu^{-}(\text{Cl}^{37}) [\text{cm}^{-1}]$
P(8)	-8	2705,75	2703,875
P(7)	-7	2730,5	2728,625
P(6)	-6	2754,75	2752,875
P(5)	-5	2778,5	2776,5
P(4)	-4	2801,75	2799,75
P(3)	-3	2824,375	2822,375
P(2)	-2	2846,375	2844,375
P(1)	-1	2867,875	2865,875

The question may arise as to what is obtained from the "depth" of the peaks (A: The ratio of the occurrence of the two Cl isotopes)
Table 8.1: Readings of the minima in the P-branch for the different isotopes

8. evaluation of task 5

Minimum	Index i	$\nu^-({}^{35}\text{Cl}) [\text{cm}]$ J^{-1}	$\nu^-({}^{37}\text{Cl}) [\text{cm}]$ J^{-1}
R(0)	1	2909,125	2907
R(1)	2	2928,75	2926,625
R(2)	3	2947,875	2945,625
R(3)	4	2966,25	2964
R(4)	5	2984	2981,75
R(5)	6	3001	2998,75
R(6)	7	3017,375	3015,125
R(7)	8	3033,125	3030,75

Table 8.2: Readings of the minima in the R-branch for the different isotopes

These data can be used to calculate the parameters vibrational wave number ν^-_s , force constant k , rotational constant B , moment of inertia I , atomic distance r_0 and strain constant D for the HCl molecule - in each case for the two isotopes ${}^{35}\text{Cl}$ and ${}^{37}\text{Cl}$.

Parameters	Isotope ${}^{35}\text{Cl}$	Isotope ${}^{37}\text{Cl}$
$\nu^-_s [\text{cm}]^{-1}$	$2888,50 \pm 1,37$	$2886,44 \pm 1,37$
$B [\text{cm}]^{-1}$	$10,31 \pm 0,69$	$10,28 \pm 0,69$
$\mu [\text{u}]$	0,9796	0,9811
$k [\text{Nm}]^{-1}$	$481,55 \pm 0,46$	$481,60 \pm 0,46$
$I [\text{kg m}]^2$	$2,72 \cdot 10^{-47} \pm 1,82 \cdot 10^{-48}$	$2,72 \cdot 10^{-47} \pm 1,83 \cdot 10^{-48}$
$r_0 [\text{m}]$	$1,29 \cdot 10^{-10} \pm 6,12 \cdot 10^{-12}$	$1,30 \cdot 10^{-10} \pm 6,15 \cdot 10^{-12}$
$D [\text{m}]^{-1}$	$0,0525 \pm 0,0086$	$0,0517 \pm 0,0085$

Table 8.3: Parameters of the HCl molecule for both isotopes

To determine the parameters B_0 , B_1 and D , the first and second order differences of the wavenumbers are plotted for the two isotopes (note: the assumption $D \approx D_0 \approx D_1$ applies).

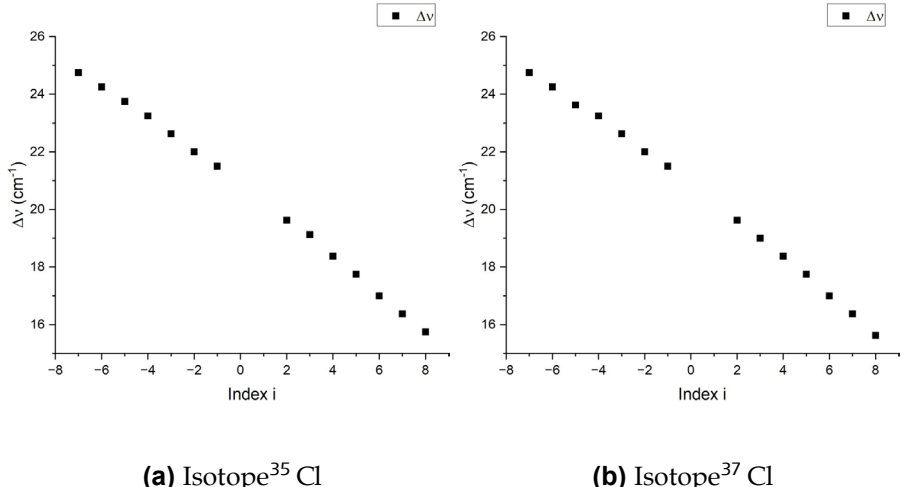


Figure 8.2: First-order differences

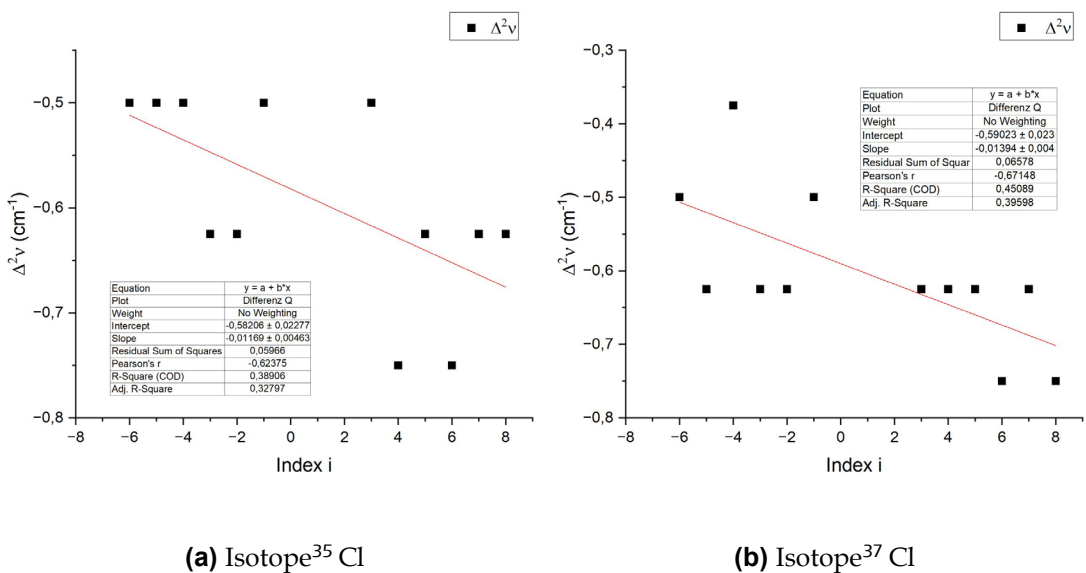


Figure 8.3: Second-order differences with linear fit

The parameter D can be calculated from the increase m using equation (1.23). The result is

$$D_{35} = -\frac{m_{35}}{24} = (0, 00049 \pm 0, 00019) \text{cm}^{-1}$$

$$D_{37} = -\frac{m_{37}}{24} = (0, 00058 \pm 0, 00017) \text{cm}^{-1}.$$

8. evaluation of task 5

This is a surprisingly accurate result in view of the large swings in the diagrams when compared with the table above. However, as expected, there are large relative errors. From the y-axis *intercept n*, the variable $B_1 - B_0$ is now obtained by

$$(B_1 - B)_{035} = -\frac{n_{35} + 24D_{35}}{2} = (-0, 297 \pm 0, 239)\text{cm}^{-1}$$
$$(B_1 - B)_{037} = -\frac{n_{37} + 24D_{37}}{2} = (-0, 401 \pm 0, 216)\text{cm}^{-1}.$$

Finally, B_0 and B_1 can be determined from the equation of the first-order difference sequence as follows

$$(B_1)_{35} = \frac{n_{35} + 4D}{2} = (10, 371 \pm 0, 019)\text{cm}^{-1}$$
$$\frac{35}{37}(B_1)_{37} = \frac{n_{37} + 4D_{37}}{2} = (10, 358 \pm 0, 020)\text{cm}^{-1},$$

with which
immediately

$$(B)_{035} = (10, 668 \pm 0, 258)\text{cm}^{-1}$$
$$(B)_{037} = (10, 759 \pm 0, 236)\text{cm}^{-1}$$

follows. However, these values should be treated with caution, as the relative errors of the values $(B_1 - B_0)$ are very large.

Their distribution was determined from the amplitudes of the peaks in the spectrum and their difference between the two isotopes. The result is that ^{35}Cl makes up about 70% of the atoms, which is a good approximation to the actual value of 75%.

9 Evaluation of task 6

To adjust the spectrum for the evaluation, the minima were first masked and the remaining data was then interpolated using the cubed B-spline method. The smoothing factor used for this is 10, and the measured spectrum was divided by this background to obtain the adjusted spectrum.

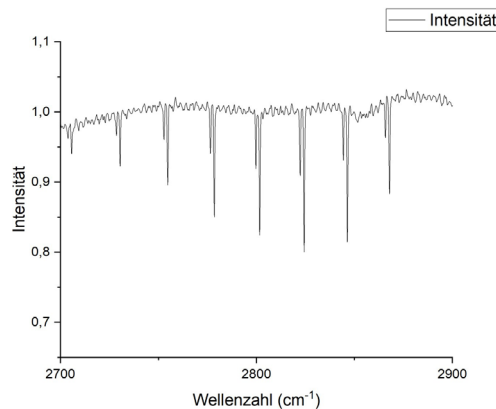


Figure 9.1: Spectrum adjusted by interpolation

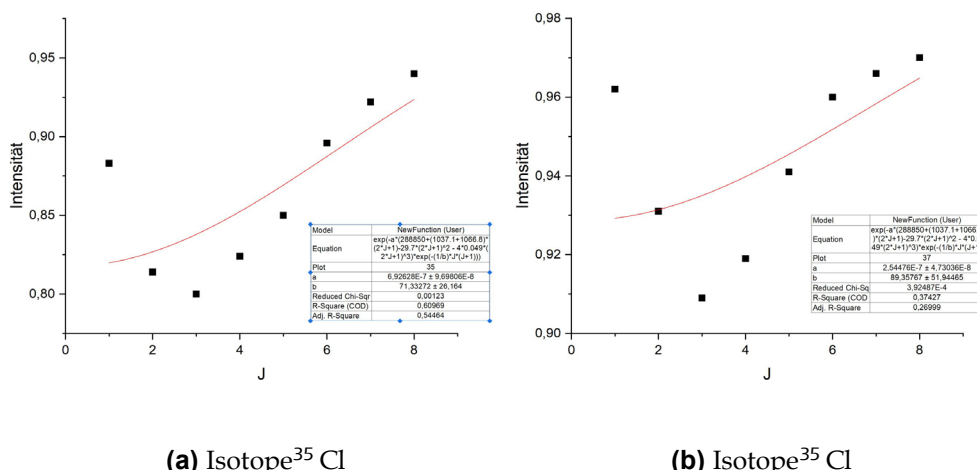


Figure 9.2: Non-linear fits for determining the temperature. These fits are obviously miserable, they should produce values close to 300K. To get a better fit (or one that converges at all), the "Initial values" in the Fit menu in Origin must be set close to the approximate expected value, then you will usually get a good fit.

9. evaluation of task 6

The intensity of the minima was plotted against the respective rotational quantum number. Equation (1.34) was used to fit both isotopes, where $\nu^-(2J + 1)$ is given by equation (1.22). The parameter b was adjusted to determine the temperature. A conversion is still necessary for this.

This results in temperatures of

$$T_{35} = (480 \pm 177)\text{K}$$

$$T_{37} = (604 \pm 351)\text{K}.$$

The diagrams already show that the fits are quite imprecise. The relative errors are correspondingly large. Temperatures of around 300 K would be expected. This is at the lower limits of both error intervals. There are errors in the measurement or the evaluation that still need to be eliminated.

10 Bibliography

T. Butz (1998): Fourier transform for pedestrians. Published by B. G. Teubner. Leipzig.

J.W. Cooley and J.W. Tukey (1965). Math. Comput.

P.S. Griffiths and J.A. de Haseth (1986): Fourier Transform Infrared Spectroscopy. John Wiley and Sons. New York.

J. Gronholz and W. Herres: Understanding FT-IR Data Processing. I and C Reprint 1(84), 3(85). Dr. Alfred Huething Publishers.

A.E. Martin (1966): Infrared Instrumentation And Techniques. Elsevier Publishing Company. Amsterdam.

V. Riede (n.d.): Rotational-vibrational spectra of molecules. University of Leipzig.

Spectrum: Fabry-Pérot interferometer. <https://www.spektrum.de/lexikon/physik/fabry-perot-interferometer/4685>. retrieved on 16.11.23